ACS OMEGA

http://pubs.acs.org/journal/acsodf

Article

Effect of Multivalency on Phase-Separated Droplets Consisting of Poly(PR) Dipeptide Repeats and RNA at the Solid/Liquid Interface

Chen Chen, Han Jia, Yoshiki Nakamura, Kohsuke Kanekura, and Yuhei Hayamizu*

Cite This: *ACS Omega* 2022, 7, 19280−19287

Read Online

ACCESS | Metrics & More | Article Recommendations | Supporting Information

ABSTRACT: Dipeptide repeat proteins (DRPs) are considered a significant cause of amyotrophic lateral sclerosis (ALS), and their liquid−liquid phase separation (LLPS) formation with other biological molecules has been studied both in vitro and in vivo. The immobilization and wetting of the LLPS droplets on glass surfaces are technically crucial for the measurement with optical microscopy. In this work, we characterized the surface diffusion of LLPS droplets of the DRPs with different lengths to investigate the multivalent effect on the interactions of their LLPS droplets with the glass surface. Using fluorescence microscopy and the single-particle tracking method, we observed that the large multivalency drastically changed the surface behavior of the droplets. The coalescence and wetting of the droplets were accelerated by increasing the multivalency of peptides in the LLPS system. Our findings on the effect of multivalency on interactions between droplets and glass surfaces could provide a new insight to enhance the understanding of LLPS formation and biophysical properties related to the solid/liquid interface.

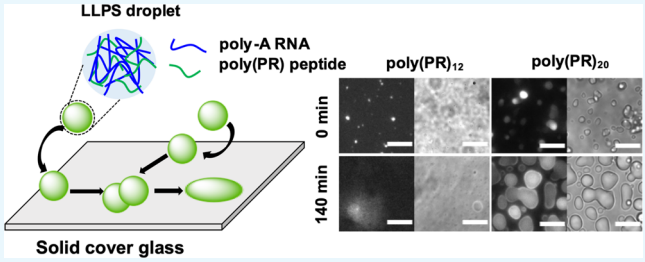

INTRODUCTION

Liquid−liquid phase separation (LLPS) has emerged as a ubiquitous physicochemical process in which solutions of biomacromolecules spontaneously separate into two liquid phases.[1,2] It has been considered to play an essential role in many fields, such as the protocell models in the origin of life research,[3,4] the formation of membraneless organelles like P granules, nucleoli,[5,6] and even the pathology of some specific neurodegenerative diseases like amyotrophic lateral sclerosis (ALS).[7−9] In principle, LLPS displays liquid-like properties with highly dynamic behaviors, where component molecules inside the droplets exhibit dynamic exchange with the surrounding environment on time scales of seconds through the interface.[10−12] The formation of LLPS is governed by synergistic intermolecular interactions, including electrostatics, cation−π, dipole−dipole, and $\pi-\pi$ interactions.[13]

It has been found that multivalency is one of the decisive factors for biological LLPS formation, which often shares the characteristics of high valency, modest affinity, and flexible connections between binding elements.[14] The multivalent effect is defined as the interaction with multiple binding sites,[15,16] and a growing body of the literature suggests that increasing valency or binding sites can lower the phase separation boundary to more dilute concentrations in their phase diagram.[1,17,18]

Arginine-rich dipeptide repeat proteins (DRPs) translated from the mutated C9orf72 gene are one of the major causes underlying ALS.[7−9,19] Poly(PR), consisting of proline and arginine, is a type of DRP. The abundant positive charges of arginine enable the poly(PR) to bind to proteins and nucleic acids at multiple sites via electrostatic forces and cation−π interactions, resulting in the formation of the LLPS droplets.[7,13,20] Their LLPS was sensitive to the multivalency of poly(PR) with lengths ranging from 6 to 60 repeats. Longer poly(PR) showed a drastic reduction in the saturation concentrations for the formation and dissolution of droplets and a reduction in the molar ratio regime of the phase separation.[20,21] The viscoelastic properties of the same LLPS droplets changed due to the poly(PR) length-dependent increases in the fluorescence recovery time for poly(PR) peptides in fluorescence recovery after photobleaching (FRAP).[21] Furthermore, the repeat lengths have also been related to the cytotoxicity of poly(PR) peptides, especially the more extended repeat tended to have a higher inhibition rate on protein synthesis.[9] These facts indicate that the multivalency of polypeptide influences its LLPS formation and even cellular functions.

To study this fundamental nature of LLPS droplets, their immobilization on the surface of transparent substrates is essential for a stable observation under optical microscopy. Recommended methods have been developed to immobilize droplets at the solid/liquid interface. The wetting assay has

Received: February 9, 2022
Accepted: May 17, 2022
Published: June 3, 2022

suggested the usage of plain glass substrates, where the spherical droplets of LLPS wet the surface and form irregular shapes over time.[22] Furthermore, it has been recommended to have a variety of coatings, e.g., poly(ethylene glycol) (PEG) or lipids, on the glass surface to preserve the material properties of droplets and have sufficiently long stability for imaging.[11] Recently, we reported that the chemically modified glass surfaces affect the diffusion of LLPS droplets and their immobilization on the glass surface.[23] This study gave us a way to control the interactions of LLPS droplets with the glass surface via the control of the net charge of the surface by the chemical modification.

As mentioned above, the multivalency of the component molecules in the LLPS is gaining more interest in the field. Thus, it is also necessary to understand how the multivalency affects the diffusion and dynamics of LLPS droplets on the surface of glass substrates. However, the understanding of the multivalency of the polypeptide and the dynamics of the LLPS droplets on the surface is still poor. In this work, we tested whether the multivalency of poly(PR) in the LLPS affects the surface behavior of the LLPS droplets. We utilized two kinds of poly(PR): $(PR)_{12}$ and $(PR)_{20}$ with a homopolymeric adenine poly-adenine (poly-A) as the model of RNA. These two peptides have different amino acid lengths, e.g., multivalency. To investigate the effect of the polypeptide multivalency on the Coulombic interaction between the LLPS droplets and solid substrate, we designed untreated cover glass and the chemically modified cover glass with positive charges. We compared the surface dynamics of LLPS droplets on glass surfaces with the single-particle tracking analysis using fluorescence microscopy.

MATERIALS AND METHODS

Reagents. Poly-A RNA was purchased from Sigma-Aldrich, and the product number was 10108626001. $(PR)_{12}$ and $(PR)_{20}$ were chemically synthesized by Genscript (Piscataway, NJ) with purity higher than 85%. In addition, trifluoroacetate was replaced by acetate.

Surface Chemical Modification. The cover glass used as a substrate (thickness No.1 0.13−0.17 mm, Matsunami Glass Ind., Ltd.) was first cleaned using plasma treatment for nearly 10 min (plasma cleaner PDC-32G, Harrick Plasma). For (3-aminopropyl)trimetoxysilane (APTMS)-modified cover glass, the substrate was immersed in 10% (3-aminopropyl)-trimethoxysilane (APTMS with nearly 97% purity, Sigma-Aldrich, in an aqueous solution for 30 min at room temperature). Afterward, the substrate was rinsed with deionized (DI) water and heated at 120 °C for 10 min. Finally, we prepared a glass surface with positively charged amine groups successfully.

LLPS Droplet Formation. We respectively mixed the solution of $(PR)_{12}$ and $(PR)_{20}$ (final concentration was 100 μM) and poly-A RNA (final concentration was 0.5 mg/mL) in the volume ratio of 1:1 in a phosphate buffer solution (final concentration was 10 mM) at room temperature. After mixing the fresh solution, we dripped 10 μL of solution on the cover glass surface and then sandwiched it with the other cover glass to form a thin solution film. As a result, the LLPS droplets were observed under an oil-immersion lens (NA = 1.4) via an inverted fluorescence microscope (Olympus IX73) with an electron-multiplying charge-coupled device (iXon-Ultra888 EMCCD, Oxford Instruments) in a bright field. The exposure time was set as 2 s, and the light source was a white light-emitting diode (LED) light positioned up the sample.

LLPS Droplet Wetting Measurement. We used the same two groups of mixture solution forming LLPS droplets. Then, we placed a poly(dimehylsiloxane) (PDMS) film (3 mm in thickness) with a hole (5 mm in diameter) on the substrate surface. The hole was filled with 20 μL of mixture solution. Meanwhile, we covered the other same cover glass on the top of the PDMS hole to avoid solution evaporation during measurement periods. To observe the wetting process of LLPS droplets on the solid interface, we defined the time scale from 0, 50, 90, and 140 min. All observations were under an oil-immersion lens (NA = 1.4) via an inverted fluorescence microscope (Olympus IX73) with an electron-multiplying charge-coupled device (iXon-Ultra888 EMCCD, Oxford Instruments) in a bright field. The exposure time was set as 2 s, and the light source was a white light-emitting diode (LED) positioned up the sample.

Fluorescence Imaging. We placed a poly-(dimethylsiloxane) (PDMS) film (3 mm in thickness) with a hole (5 mm in diameter) on the substrate surface. $(PR)_{12}$ and $(PR)_{20}$ (final concentration of 100 μM) were respectively mixed with poly-A RNA (final concentration was 0.5 mg/mL, M_W = 100−500 kDa) in the volume ratio of 1:1 in a phosphate buffer solution (final concentration of 10 mM) in the tube at room temperature. The hole was filled with 20 μL of mixture solution. Meanwhile, we covered the other same cover glass on the top of the PDMS hole to avoid solution evaporation during measurement periods. To observe the interaction of LLPS droplets with the solid interface, we utilized an inverted fluorescence microscope (IX73P2F, Olympus, JP) with a fluorescence filter cube (emission: 420−460 nm; excitation: >515 nm). A mercury lamp was utilized as an input power (7 mW) to excite the fluorescent dye. The sample was then put on the fluorescence microscope equipped with an oil-immersion lens (NA = 1.4) and a complementary metal-oxide semiconductor (CMOS) camera (Neo sCMOS/Solis, Andor, JP). A series of fluorescence images were recorded continuously to investigate the interaction between the LLPS droplets and the solid glass surface with an exposure time of 10 ms.

FRAP Analysis. Each poly(PR) peptide (final concentration was 100 μM) and poly-A RNA (final concentration was 0.5 mg/mL) containing 100 nM of tetramethylrhodamine (TAMRA)-A_{15} was mixed at room temperature. The droplets were observed on an untreated cover glass via LSM-710 confocal microscopy with a water-immersion 60× lens of NA 1.2. The FRAP results were analyzed with Zen software (Carl Zeiss).

Single-Particle Tracking. We utilized an open-source platform for biological-image processing software Fiji with a plug-in for multiple particle detection and tracking to automatically identify the density center of fluorescent dots from the obtained fluorescence images and then extract the location of LLPS droplets on the solid surface. The trajectories of the droplet were obtained by linking the nearest position in consecutive frames. The coordinates of the LLPS droplet can be obtained using single-particle tracking methods. Consequently, we measured the total fluorescence intensity of the single LLPS droplet and analyzed the mean square displacement.

RESULTS AND DISCUSSION

LLPS Droplet Formation on the Substrate. We formed LLPS droplets by mixing $(PR)_{12}$ and $(PR)_{20}$ separately with

https://doi.org/10.1021/acsomega.2c00811
ACS Omega 2022, 7, 19280−19287

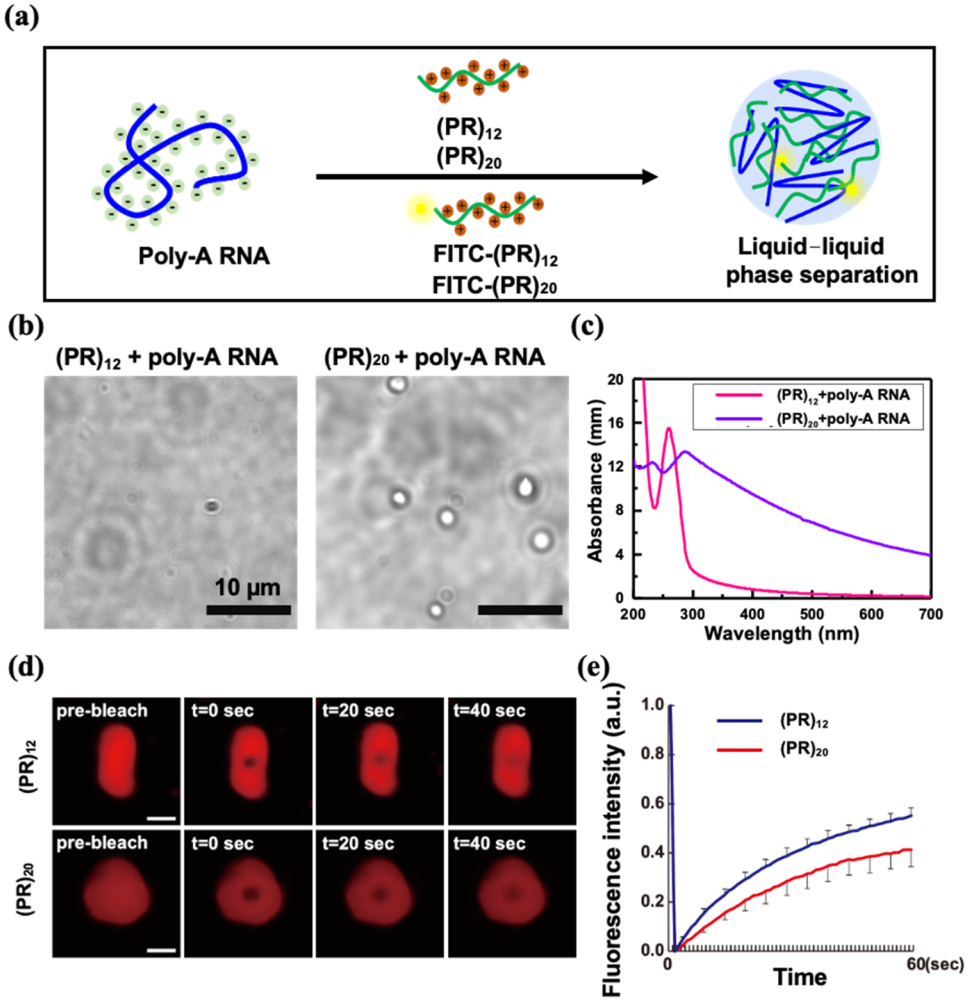

Figure 1. LLPS formation and characterization in the bulk solution. (a) LLPS droplet formation involving poly-A RNA, $(PR)_{12}$, and FITC-$(PR)_{12}$; poly-A RNA, $(PR)_{20}$, and FITC-$(PR)_{20}$. (b) Optical transmission images of LLPS in the phosphate buffer solution. Scale bar: 10 μm. (c) Optical absorbance spectra of each mixture solution showing the light scattering effect due to the LLPS droplet formation. (d) Fluorescence images of each LLPS droplet under the FRAP measurements. Scale bar: 10 μm. (e) FRAP for each peptide with 5 times for each measurement.

poly-adenine (poly-A) RNA (Figure 1a). A fraction of poly(PR) labeled with fluorescein isothiocyanate (FITC) was also introduced into the samples for fluorescence measurement. The final mixture solution became opalescent at an optimized solution concentration and mixing volume ratio. Optical microscopy revealed the presence of numerous spherical droplets, indicating the phase separation of the solution (Figure 1b). Much larger droplets of $(PR)_{20}$ than those of $(PR)_{12}$ mixed with poly-A. We also conducted the optical absorption measurements at the wavelength of 500 nm for the droplets in a phosphate buffer solution using a nanophotometer (Implen NanoPhotometer, N60) to characterize the mixture solution turbidity. The absorption spectra showed that the absorption of the two LLPS groups had a significant increase because of the light scattering from the LLPS droplet formation (Figure 1c) compared with their respective individual components like polypeptide and RNA solution (Figure S1). Usually, the light reflection phenomenon from internal interfaces is partially regarded as the difference in the refractive indexes of different structures within a complex medium, leading to the scattering component formation. We found that the distortion tail of the absorbance curve for LLPS containing $(PR)_{20}$ is much longer than that containing $(PR)_{12}$. The light scattering seen in the absorbance spectra of Figure 1 indicates that $(PR)_{20}$ had a greater number of LLPS droplets than $(PR)_{12}$. It implies that polypeptide with larger multivalency tends to form a higher number density of the LLPS droplets in the bulk solution, which agrees with the results of the optical microscopy in Figure 1b. It is also consistent with a previous report.[20] Furthermore, we performed fluorescence recovery after photobleaching (FRAP) to evaluate the fluidity of the peptides in the LLPS droplets (Figure 1d). The fluorescence recovery was found to be more significant in the case of $(PR)_{12}$ than in $(PR)_{20}$ (Figure 1e), indicating that the larger multivalency causes more viscous droplets. The recovery time constants for both peptides were almost equivalent. This indicates that a fraction of poly-A is hardly mobile in the droplets.

Next, we utilized fluorescence microscopy to investigate the diffusion of LLPS droplets of $(PR)_{12}$ and $(PR)_{20}$ mixed with poly-A RNA on two solid substrate surfaces. One is an untreated cover glass and the other is a (3-aminopropyl)-trimetoxysilane (APTMS)-modified cover glass with positively charged amino groups (Figure 2a).[24] Through the automatic contact angle meter (Simage AUTO 100), we performed contact angle measurements with DI water to evaluate the

https://doi.org/10.1021/acsomega.2c00811
ACS Omega 2022, 7, 19280−19287

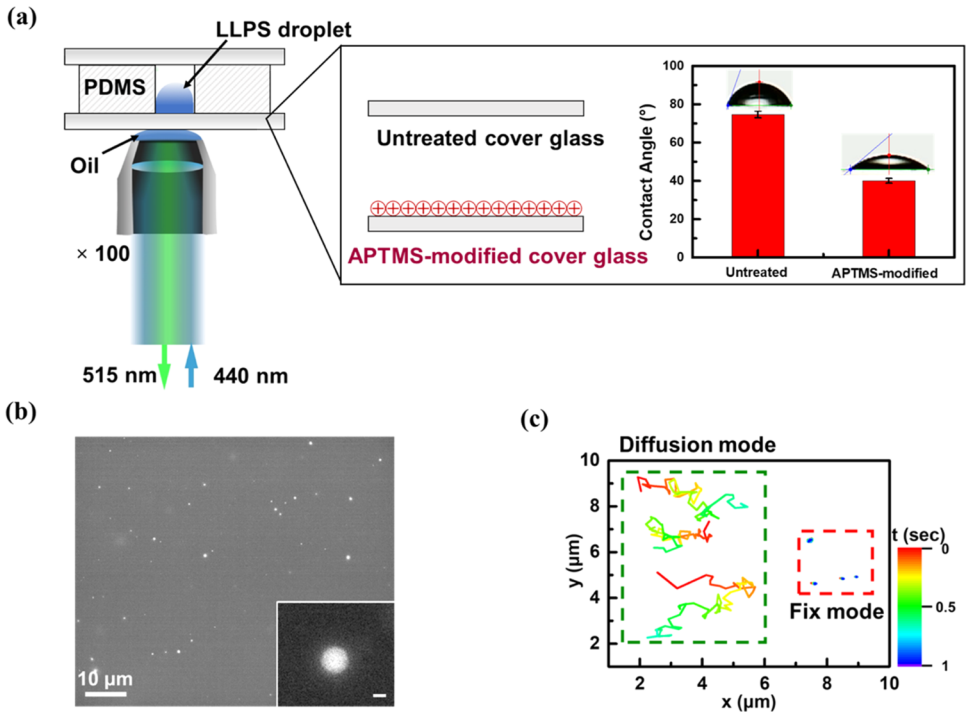

Figure 2. LLPS droplet detection at the solid/liquid interface by a fluorescence microscope. (a) Schematic illustration detecting the interaction between the LLPS droplet and the solid surface via a fluorescence microscope. The solid surfaces were an untreated cover glass and APTMS-modified cover glass and the measurement of the contact angle for each of them. (b) Fluorescence image showing LLPS droplets on the solid surface. Scale bar: 10 μm (inset image: scale bar: 1 μm). (c) Representative trajectories of the observed LLPS with a color scale of the observation time.

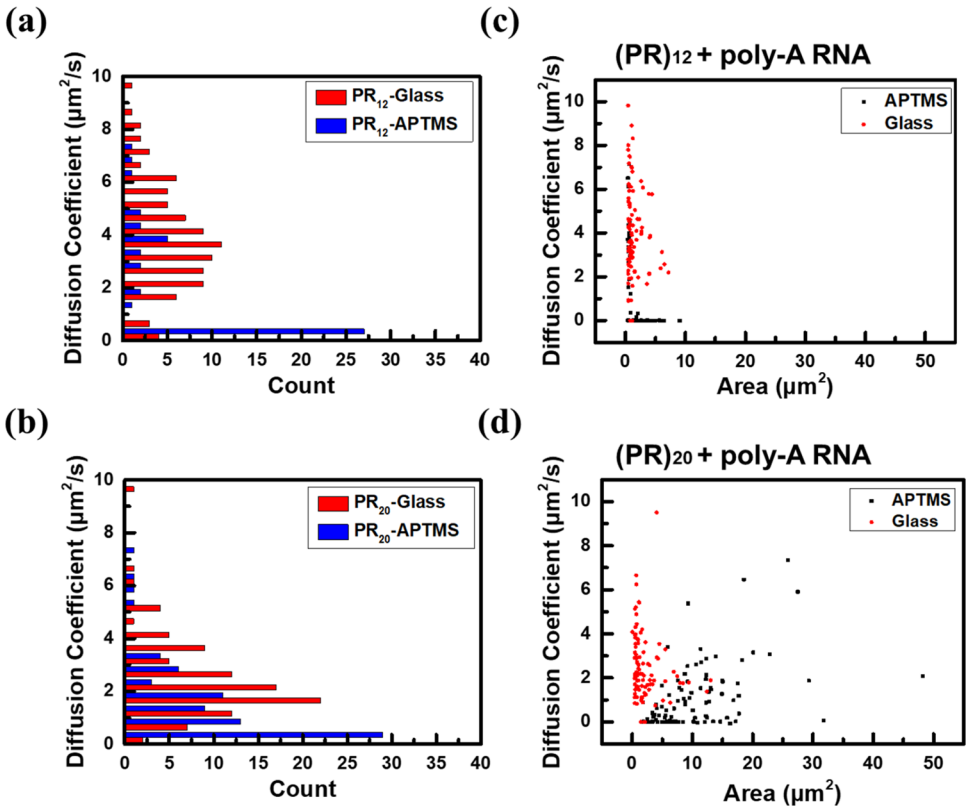

Figure 3. (a, b) Estimation of the diffusion coefficient for LLPS droplets formed by $(PR)_{12}$ and poly-A RNA in a phosphate buffer solution and $(PR)_{20}$ and poly-A RNA in a phosphate buffer solution at two substrates. (c, d) Scattered plots showing the relationship between the area and the diffusion coefficient of LLPS droplets in two cases.

https://doi.org/10.1021/acsomega.2c00811
ACS Omega 2022, 7, 19280−19287

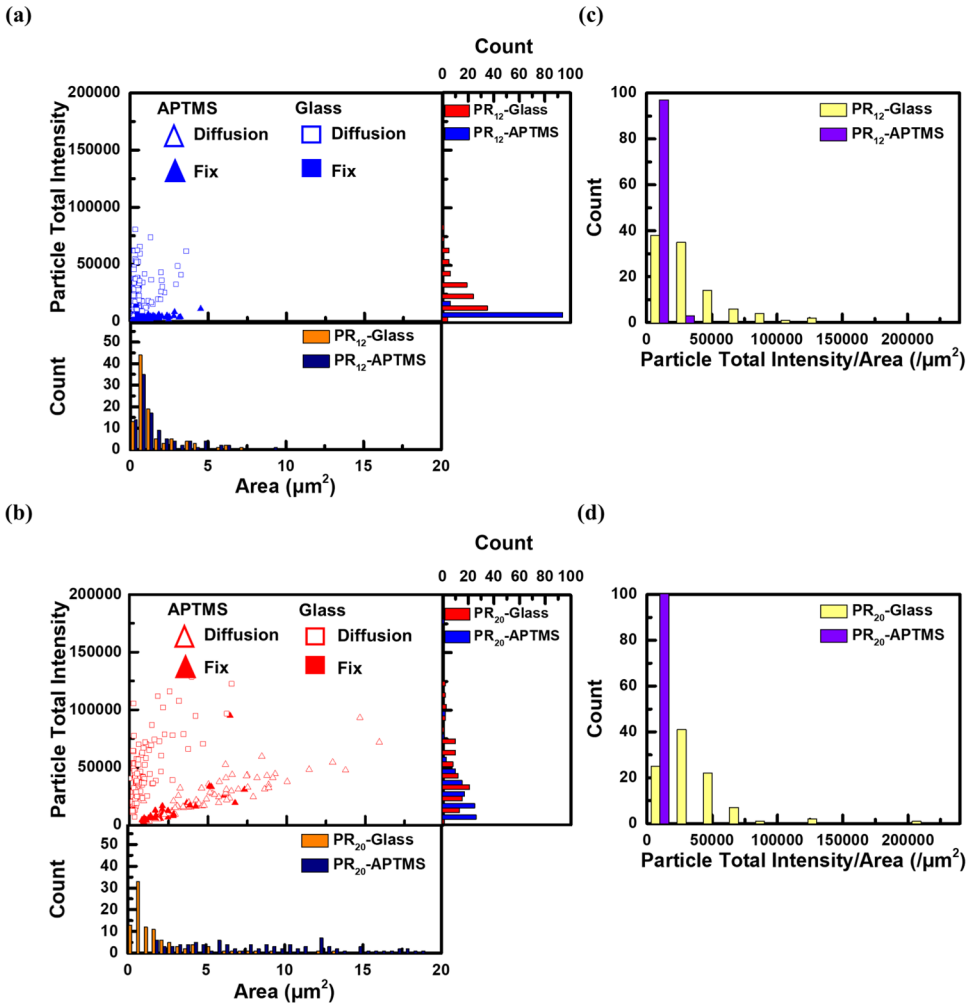

Figure 4. (a, b) Scattered plots showing the relationship between the area and the fluorescent intensity of droplets formed by $(PR)_{12}$ and poly-A RNA and $(PR)_{20}$ and poly-A RNA in a phosphate buffer solution at two substrates. (c, d) Count of particle total intensity per area in the former two cases.

water wettability on both substrates. The results indicate that the APTMS-modified cover glass surface is more hydrophilic with a contact angle of nearly 40.1° than untreated cover glass with a contact angle of nearly 74.7° (Figure 2a). A fraction of poly(PR) was labeled with FITC. The fluorescence from the LLPS droplets was detected through the Fiji single-particle tracking analysis, an open-source platform for biological-image processing.[25,26] After recording the fluorescent images of the LLPS droplets on an untreated glass surface (Figure 2b), we plotted the trajectories of some typical cases and their displacement with time (Figure 2c). All trajectories can be categorized into (1) fix mode with small displacements and (2) diffusion mode with much longer displacements during the same time range.

Surface Diffusion of the LLPS Droplet. To investigate the multivalency effect on LLPS droplets surface dynamics on the untreated cover glass surface and APTMS-modified cover glass surface, we analyzed their mean square displacement (MSD) quantitatively.[27] The MSD was derived using the following equation[28]

$$\mathrm{MSD}(\Delta t) = \langle \Delta r(\Delta t)^2 \rangle = \langle (r(t+\Delta t) - r(t))^2 \rangle = 4D \cdot \Delta t \quad (1)$$

where Δr is the displacement of the particle, t is the time of diffusion, and Δt is the lag time between two images. This equation is applicable in the case of two-dimensional Brownian motion.[29] Figure S2 shows the MSD results from the trajectories of 100 groups of LLPS droplets individually diffused on an untreated cover glass or an APTMS-modified cover glass. For LLPS with $(PR)_{12}$, the diffusion of the most LLPS droplets followed the two-dimensional Brownian motion since MSD increases linearly with Δt and a small number of droplets revealed the fixed mode on the untreated glass surface. In contrast, the APTMS-modified glass surface exhibited a small number of droplets following the two-dimensional Brownian motion. These results are consistent with our previous report.[23]

In the case of the $(PR)_{20}$, the tendency in their MSD was different from that of $(PR)_{12}$. First, the slope of the MSD was slower than $(PR)_{12}$ on average. Second, most droplets of $(PR)_{20}$ revealed a longer diffusion duration on the surface, while LLPS droplets with $(PR)_{12}$ frequently came off from the surface. According to the MSD results (Figure S2), we found that MSD showed linearity in the time of less than 0.1 s and nonlinearity in the time longer than 0.1 s. The nonlinearity is probably due to interactions among LLPS droplets or specific interactions with the surface-immobilizing LLPS droplets for a

https://doi.org/10.1021/acsomega.2c00811
ACS Omega 2022, 7, 19280−19287

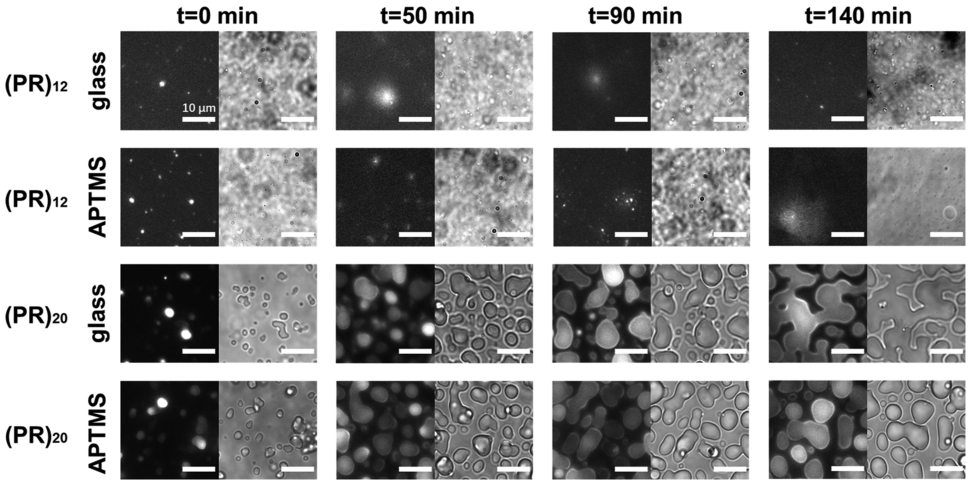

Figure 5. Time lapse of fluorescence images (left) and transmission images (right) of LLPS droplets consisting of $(PR)_{12}$ or $(PR)_{20}$ on the untreated cover glass surface and APTMS-modified cover glass surface. All the scale bar is 10 μm.

short time. The diffusion of the LLPS droplets at the solid/liquid interface could be the switching between diffusion and immobilization mode.[23] To this end, we utilized the linear region of MSD with a time range of less than 0.1 s to estimate the diffusion coefficients for LLPS droplets. For a quantitative comparison between these two peptides, we derived the diffusion coefficients of LLPS droplets on the glass surfaces by fitting with eq 1. We assumed that all LLPS droplets followed the two-dimensional random diffusion at the interfaces. The derived diffusion coefficients of all droplets observed in the measurement were plotted in the form of a histogram (Figure 3a,b). Consistent with the observations in the previous study,[23] PR_{12} showed a clear difference between the untreated and APTMS-modified glasses. While LLPS droplets diffused on the surface of the untreated glass, most droplets were immobilized on the APTMS-modified glass. This phenomenon could be explained by the negative ζ-potential of LLPS droplets of PR dipeptide and poly-RNA, and we assumed that positively charged amino groups of the APTMS on the glass surface attracted the LLPS droplets due to the attractive electrostatic interaction.[23,30] The diffusion coefficient for LLPS with $(PR)_{12}$ was widely distributed, and most droplets were in motion on the untreated cover glass surface. We defined these two modes of droplet diffusion as fixed and diffusion modes, respectively.

The multivalency of PR can be examined by comparing the results of $(PR)_{12}$ with those of $(PR)_{20}$. The histogram of $(PR)_{20}$ exhibited that $(PR)_{20}$ had smaller diffusion coefficients than $(PR)_{12}$ on average on both surfaces of untreated and APTMS-modified glass. Interestingly, $(PR)_{20}$ also showed some droplets immobilized on the APTMS-modified glass with a limited portion, but most of them diffused on the surface. The variation in the diffusion coefficients among the peptides may be explained by the difference in their intermolecular interactions and interactions with the surface. We plotted the diffusion coefficient of each droplet as a dependence of the areal size of the droplets on the surface (Figure 3c,d). The areal size of $(PR)_{12}$ was distributed within less than 10 μm^2 in both untreated and APTMS-modified glass. $(PR)_{20}$ showed the size less than 10 μm^2 in the case of untreated surface, but the size exceeded more than 10 μm^2 in the case of the APTMS-modified glass. It indicates that $(PR)_{20}$ tended to form larger droplets and have lower diffusion coefficients than $(PR)_{12}$, which may be related to the multivalency of the peptides.

To further understand the multivalency effect on the surface diffusion, the relationship between the averaged area and total fluorescence intensity of each droplet is plotted in Figure 4a,b. For both plots, the data points with filled and blank makers represent the results of droplets in fix and diffusion modes, respectively. $(PR)_{12}$ showed a clear difference in the distribution of data points between the fix and diffusion modes. The fix mode had low total intensities of less than 10 000. The diffusion mode exhibited that the average area ranged less than 5 μm^2 in the case of the untreated glass surface. Moreover, the total intensity ranged up to 75 000 (Figure 4a).

On the other hand, $(PR)_{20}$ showed a wider distribution than $(PR)_{12}$ in Figure 4b. The droplets on the APTMS-modified glass tended to have a larger area than those on the untreated glass. These data points revealed two groups with distinct individual slopes, where data points on APTMS-modified glass have a slower slope and ones on untreated glass have a steeper slope. The slope, e.g., the ratio between the total intensity and the area, could be related to the thickness of the droplets on the surface by assuming that the total intensity is roughly proportional to the volume of the droplet. We plotted the distribution of the ratio in Figure 4c,d for both $(PR)_{12}$ and $(PR)_{20}$. As seen in the two groups with distinct slopes, we can find a clear difference between the untreated and APTMS-modified glass. For both $(PR)_{12}$ and $(PR)_{20}$, the untreated glass showed a larger ratio than the APTMS-modified glass, indicating that the thickness of the droplets on the APTMS-modified glass was thinner than that of the untreated glass. This is probably due to the difference in the wetting of droplets on the surface. It is also noted that the peak position of $(PR)_{20}$ was slightly right-shifted compared with one of $(PR)_{12}$, indicating that $(PR)_{20}$ tended to have slightly thicker droplets on the untreated surface. In addition, the fluorescence intensity difference between the peptides might arise from the distinct efficiency of incorporating the TAMRA-labeled RNA into the droplets. In the above analysis, we assume the efficiency difference was ignorable.

In the light of the above results in Figures 3 and 4, the multivalency of the polypeptide seems to affect the diffusion of the LLPS droplets on the surface in two ways: (1) polypeptides with a larger multivalency result in the formation of larger droplets, (2) $(PR)_{20}$ has a more fraction of the diffusion mode

https://doi.org/10.1021/acsomega.2c00811
ACS Omega 2022, 7, 19280−19287

even on the APTMS-modified glass. It indicates that the intermolecular interactions among the polypeptides and poly-A are relatively more dominant than the interactions with the surface during the droplet diffusion. From these points of view, we next focus on the coalescence of the LLPS droplets on the surface, on which the multivalency of polypeptides may have an impact.

Coalescence and Wetting of the LLPS Droplet at the Solid/Liquid Interface. The same LLPS droplets as those mentioned above were observed on both untreated and APTMS-modified glass surfaces for longer durations. It has been reported that the droplets have characteristics of a liquid phase with distinct wetting behavior after prolonged incubation and fusion upon making contact.[31] We, therefore, set the incubation time for LLPS droplets on different substrate surfaces ranging from 0, 50, 90, to 140 min and took the fluorescence and transmission images, respectively, to record the morphology of the LLPS droplets. As shown in Figure 5, $(PR)_{20}$ tended to accelerate the LLPS droplets wetting and coalescence during the incubation process, while $(PR)_{12}$ did not show the coalescence, neither on the untreated cover glass surface or APTMS-modified cover glass surface. These results are consistent with those in Figures 3 and 4 where droplets of $(PR)_{20}$ revealed a larger area than $(PR)_{12}$ on average.

CONCLUSIONS

In summary, we investigated the effect of multivalency on the LLPS droplet diffusion and dynamics at the solid/liquid interface. We compared the LLPS droplets formed by $(PR)_{12}$ and $(PR)_{20}$ on the glass surfaces and found that they have both fix and diffusion modes on the untreated cover glass surface and chemically modified cover glass surface with positive charges, respectively. Moreover, $(PR)_{20}$ tended to form larger droplets with smaller diffusion coefficients. The multivalency of the polypeptides showed enrichments for both wetting and coalescence of their droplets on the glass surface. This work could be helpful for understanding the LLPS formation and biophysical properties through optical experiments at solid/liquid interfaces.

ASSOCIATED CONTENT

Supporting Information

The Supporting Information is available free of charge at https://pubs.acs.org/doi/10.1021/acsomega.2c00811.

Optical absorbance at 500 nm for mere poly-A RNA, $(PR)_{20}$, and $(PR)_{12}$ solutions. Mean square distribution (MSD) of the LLPS droplets consisting of $(PR)_{20}$ or $(PR)_{12}$ diffusion on the untreated cover glass and APTMS-modified cover glass surface (PDF)

AUTHOR INFORMATION

Corresponding Author

Yuhei Hayamizu − *Department of Materials Science and Engineering, School of Materials and Chemical Technology, Tokyo Institute of Technology, Tokyo 152-8550, Japan;* orcid.org/0000-0003-1411-9400; Email: hayamizu.y.aa@m.titech.ac.jp

Authors

Chen Chen − *Department of Materials Science and Engineering, School of Materials and Chemical Technology, Tokyo Institute of Technology, Tokyo 152-8550, Japan*

Han Jia − *Department of Materials Science and Engineering, School of Materials and Chemical Technology, Tokyo Institute of Technology, Tokyo 152-8550, Japan*

Yoshiki Nakamura − *Department of Materials Science and Engineering, School of Materials and Chemical Technology, Tokyo Institute of Technology, Tokyo 152-8550, Japan*

Kohsuke Kanekura − *Department of Molecular Pathology, Tokyo Medical University, Tokyo 160-8402, Japan;* orcid.org/0000-0002-2901-9595

Complete contact information is available at: https://pubs.acs.org/10.1021/acsomega.2c00811

Notes

The authors declare no competing financial interest.

ACKNOWLEDGMENTS

This work was partly supported by the JSPS 20H03593.

REFERENCES

(1) Banani, S. F.; Lee, H. O.; Hyman, A. A.; Rosen, M. K. Biomolecular Condensates: Organizers of Cellular Biochemistry. *Nat. Rev. Mol. Cell Biol.* **2017**, *18*, 285−298.

(2) Bracha, D.; Walls, M. T.; Brangwynne, C. P. Probing and Engineering Liquid Phase Organelles. *Nat. Biotechnol.* **2019**, *37*, 1435−1445.

(3) Jia, T. Z.; Caudan, M.; Mamajanov, I. Origin of Species before Origin of Life: The Role of Speciation in Chemical Evolution. *Life* **2021**, *11*, No. 154.

(4) Jia, T. Z.; Bapat, N. V.; Verma, A.; Mamajanov, I.; Cleaves, H. J.; Chandru, K. Incorporation of Basic α-Hydroxy Acid Residues into Primitive Polyester Microdroplets for RNA Segregation. *Biomacromolecules* **2021**, *22*, 1484−1493.

(5) Hyman, A. A.; Brangwynne, C. P. Beyond Stereospecificity: Liquids and Mesoscale Organization of Cytoplasm. *Dev. Cell* **2011**, *21*, 14−16.

(6) Hyman, A. A.; Weber, C. A.; Jülicher, F. Liquid−Liquid Phase Separation in Biology. *Annu. Rev. Cell Dev. Biol.* **2014**, *30*, 39−58.

(7) Chen, C.; Yamanaka, Y.; Ueda, K.; et al. Phase Separation and Toxicity of C9ORF72 Poly(PR) Depends on Alternate Distribution of Arginine. *J. Cell Biol.* **2021**, *220*, No. e202103160.

(8) Kanekura, K.; Yagi, T.; Cammack, A. J.; Mahadevan, J.; Kuroda, M.; Harms, M. B.; Miller, T. M.; Urano, F. Poly-Dipeptides Encoded by the C9ORF72 Repeats Block Global Protein Translation. *Hum. Mol. Genet.* **2016**, *25*, 1803−1813.

(9) Kanekura, K.; Harada, Y.; Fujimoto, M.; Yagi, T.; Hayamizu, Y.; Nagaoka, K.; Kuroda, M. Characterization of Membrane Penetration and Cytotoxicity of C9orf-72-Encoding Arginine-Rich Dipeptides. *Sci. Rep.* **2018**, *8*, No. 12740.

(10) Wang, Z.; Zhang, G.; Zhang, H. Protocol for Analyzing Protein Liquid−Liquid Phase Separation. *Biophys. Rep.* **2019**, *5*, 1−9.

(11) Alberti, S.; Saha, S.; Woodruff, J. B.; Franzmann, T. M.; Wang, J.; Hyman, A. A. A User's Guide for Phase Separation Assays with Purified Proteins. *J. Mol. Biol.* **2018**, *430*, 4806−4820.

(12) Lin, Y.; Mori, E.; Kato, M.; Xiang, S.; Wu, L.; Kwon, I.; McKnight, S. L. Toxic PR Poly-Dipeptides Encoded by the C9orf72 Repeat Expansion Target LC Domain Polymers. *Cell* **2016**, *167*, 789−802.e12.

(13) Boeynaems, S.; Holehouse, A. S.; Weinhardt, V.; Kovacs, D.; Van Lindt, J.; Larabell, C.; Van Den Bosch, L.; Das, R.; Tompa, P. S.; Pappu, R. V.; Gitler, A. D. Spontaneous Driving Forces Give Rise to Protein-RNA Condensates with Coexisting Phases and Complex

Material Properties. *Proc. Natl. Acad. Sci. U.S.A.* **2019**, *116*, 7889−7898.
(14) Jin, J.; Xie, X.; Chen, C.; Park, J. G.; Stark, C.; James, D. A.; Olhovsky, M.; Linding, R.; Mao, Y.; Pawson, T. Eukaryotic Protein Domains as Functional Units of Cellular Evolution. *Sci. Signaling* **2009**, *2*, No. ra76.
(15) Shin, Y.; Brangwynne, C. P. Liquid Phase Condensation in Cell Physiology and Disease. *Science* **2017**, *357*, No. eaaf4382.
(16) Zumbro, E.; Alexander-Katz, A. Influence of Binding Site Affinity Patterns on Binding of Multivalent Polymers. *ACS Omega* **2020**, *5*, 10774−10781.
(17) Li, P.; Banjade, S.; Cheng, H. C.; Kim, S.; Chen, B.; Guo, L.; Llaguno, M.; Hollingsworth, J. V.; King, D. S.; Banani, S. F.; Russo, P. S.; Jiang, Q. X.; Nixon, B. T.; Rosen, M. K. Phase Transitions in the Assembly of Multivalent Signalling Proteins. *Nature* **2012**, *483*, 336−340.
(18) Harmon, T. S.; Holehouse, A. S.; Rosen, M. K.; Pappu, R. V. Intrinsically Disordered Linkers Determine the Interplay between Phase Separation and Gelation in Multivalent Proteins. *eLife* **2017**, *6*, No. e30294.
(19) Nedelsky, N. B.; Taylor, J. P. Bridging Biophysics and Neurology: Aberrant Phase Transitions in Neurodegenerative Disease. *Nat. Rev. Neurol.* **2019**, *15*, 272−286.
(20) Boeynaems, S.; Bogaert, E.; Kovacs, D.; Konijnenberg, A.; Timmerman, E.; Volkov, A.; Guharoy, M.; De Decker, M.; Jaspers, T.; Ryan, V. H.; Janke, A. M.; Baatsen, P.; Vercruysse, T.; Kolaitis, R. M.; Daelemans, D.; Taylor, J. P.; Kedersha, N.; Anderson, P.; Impens, F.; Sobott, F.; Schymkowitz, J.; Rousseau, F.; Fawzi, N. L.; Robberecht, W.; Van Damme, P.; Tompa, P.; Van Den Bosch, L. Phase Separation of C9orf72 Dipeptide Repeats Perturbs Stress Granule Dynamics. *Mol. Cell* **2017**, *65*, 1044−1055.e5.
(21) White, M. R.; Mitrea, D. M.; Zhang, P.; Stanley, C. B.; Cassidy, D. E.; Nourse, A.; Phillips, A. H.; Tolbert, M.; Taylor, J. P.; Kriwacki, R. W. C9orf72 Poly(PR). Dipeptide Repeats Disturb Biomolecular Phase Separation and Disrupt Nucleolar Function. *Mol. Cell* **2019**, *74*, 713−728.e6.
(22) Wang, Z.; Zhang, G.; Zhang, H. Protocol for Analyzing Protein Liquid−Liquid Phase Separation. *Biophys. Rep.* **2019**, *5*, 1−9.
(23) Chen, C.; Li, P.; Luo, W.; Nakamura, Y.; Dimo, V. S.; Kanekura, K.; Hayamizu, Y. Diffusion of LLPS Droplets Consisting of Poly(PR) Dipeptide Repeats and RNA on Chemically Modified Glass Surface. *Langmuir* **2021**, *37*, 5635−5641.
(24) Wang, Y. Q.; Xu, S. B.; Deng, J. G.; Gao, L. Z. Enhancing the Efficiency of Planar Heterojunction Perovskite Solar Cells via Interfacial Engineering with 3-Aminopropyl Trimethoxy Silane Hydrolysate. *R. Soc. Open Sci.* **2017**, *4*, No. 170980.
(25) Saxton, M. J. Single-Particle Tracking: Connecting the Dots. *Nat. Methods* **2008**, *5*, 671−672.
(26) Schindelin, J.; Arganda-Carreras, I.; Frise, E.; Kaynig, V.; Longair, M.; Pietzsch, T.; Preibisch, S.; Rueden, C.; Saalfeld, S.; Schmid, B.; Tinevez, J. Y.; White, D. J.; Hartenstein, V.; Eliceiri, K.; Tomancak, P.; Cardona, A. Fiji: An Open-Source Platform for Biological-Image Analysis. *Nat. Methods* **2012**, *9*, 676−682.
(27) Savin, T.; Doyle, P. S. Static and Dynamic Errors in Particle Tracking Microrheology. *Biophys. J.* **2005**, *88*, 623−638.
(28) Manzo, C.; Garcia-Parajo, M. F. A Review of Progress in Single Particle Tracking: From Methods to Biophysical Insights. *Rep. Prog. Phys.* **2015**, *78*, No. 124601.
(29) H, C. *Random Walks in Biology*; Princeton University Press, 1993.
(30) Welsh, T. J.; Krainer, G.; Espinosa, J.; Joseph, J.; Sridhar, A.; Jahnel, M.; Arter, W.; Saar, K.; Alberti, S.; Collepardo-Guevara, R.; Knowles, T. P. J. Surface Electrostatics Govern the Emulsion Stability of Biomolecular Condensates. *Nano Lett.* **2022**, *22*, 612−621.
(31) Hardenberg, M.; Horvath, A.; Ambrus, V.; Fuxreiter, M.; Vendruscolo, M. Widespread Occurrence of the Droplet State of Proteins in the Human Proteome. *Proc. Natl. Acad. Sci. U.S.A.* **2020**, *117*, 33254−33262.

https://doi.org/10.1021/acsomega.2c00811
ACS Omega 2022, 7, 19280−19287